The Diabatic Deacon Cell*

KEVIN SPEER

Department of Oceanography, The Florida State University, Tallahassee, Florida

STEPHEN R. RINTOUL

CSIRO Marine Research and Antarctic CRC, Hobart, Australia

BERNADETTE SLOYAN

Alfred Wegener Institute, Bremerhaven, Germany

(Manuscript received 30 July 1999, in final form 23 February 2000)

ABSTRACT

Southern Ocean air–sea fluxes from the COADS dataset are examined for compatibility between buoyancy gain and northward Ekman transport. An analysis in density classes points to an upwelling of Upper Circumpolar Deep Water and subsequent buoyancy gain from air–sea exchange as water flows northward in the Ekman layer. The Upper Circumpolar Deep Water layer is too shallow to admit southward geostrophic flow along topography, and an eddy mass flux mechanism for southward transport in this layer to replenish the upwelling is advanced, based on observed large-scale potential vorticity gradients. Estimates of the strength and vertical structure of the meridional flow are given using repeated hydrographic sections and a new climatology.

1. Introduction

The meridional circulation of the Southern Ocean is often described as a Deacon cell, in which deep water upwells, is blown north by wind stress in an Ekman layer, and sinks at the Antarctic convergence (Fig. 1: Sverdrup et al. 1942; Toggweiler and Samuels 1993; Tomczak and Godfrey 1994). The conception of the Deacon cell was based on the idea of a transformation of water from cold, dense layers to warmer, lower density layers. A second, deeper, cell is associated with bottom-water formation, sinking, and entrainment next to the Antarctic continent, equatorward flow near the bottom, and the southward inflow of deep water. Thus, deep inflow must compensate both near-bottom and near-surface northward outflow; this deep inflow is thought to be accomplished geostrophically since ridges provide lateral boundaries that support east–west pressure gradients below their crests.

That buoyancy loss is required to form dense bottom water is evident, although the distribution and strength of this loss is poorly known. Similarly, the Deacon cell apparently requires a buoyancy gain, but this aspect has received little attention, partly because a high-latitude ocean is naturally expected to lose heat (though this does not guarantee buoyancy loss) and partly because the air–sea flux data are sparse in the Southern Ocean.

Surface temperatures within the Antarctic divergence increase from roughly 1°–3°C to about 4°C at the Polar Front. The northward Ekman transport apparently crosses these mean sea surface isotherms, and this increase in temperature of water moving north across the front led Toole (1981) to infer oceanic heat gain south of the Polar Front. Warren et al. (1996) emphasized the compatibility between a buoyancy input and the Deacon cell, and concluded that sufficient buoyancy gain exists to balance a northward Ekman transport of 11 Sv (Sv $\equiv$ 10^6 m^3 s^{-1}) at 60°S. Their data sources implied that the net buoyancy gain at this latitude is the result of a very weak buoyancy loss due to cooling plus a stronger gain from the freshwater flux. Taylor et al. (1978) noted that in the Atlantic and Australian sectors at latitudes roughly south of the Polar Front, the data implied a net heat gain, not loss, suggesting rather stronger buoyancy input. They argued that this situation could result from north–south excursions of atmospheric and oceanic frontal systems. Regardless of the mechanism, the northward Ekman flow across mean surface isotherms or is-

* Alfred Wegener Institute Contribution Number 1657.

Corresponding author address: Dr. Kevin G. Speer, Department of Oceanography, The Florida State University, Tallahassee, FL 32306-4320.
E-mail: kspeer@ocean.fsu.edu

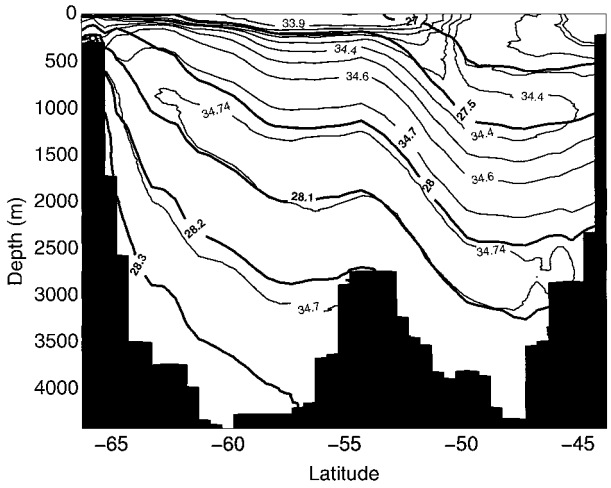

FIG. 1. Average salinity (psu) from six WOCE SR3 repeat sections from Tasmania to Antarctica. Heavy lines show surfaces of constant neutral density anomaly (kg m^{-3}), dividing the section roughly into water mass layers (AAIW: 27–27.5, UCDW: 27.5–28, LCDW or NADW: 28–28.2, and AABW below 28.2). A salinity maximum in the NADW rising to the south and a salinity minimum AAIW descending to the north is suggestive of a meridional circulation cell (Deacon 1937).

opycnals requires a net heat gain. Our COADS data (da Silva et al. 1994) shows buoyancy gain to be a more extensive phenomenon with the strongest area of buoyancy gain centered in the Indian Ocean sector south of Africa; greater buoyancy gain is consistent with the stronger northward Ekman transport in the COADS winds.

Without any surface buoyancy forcing at all, Döös (1994) has modeled the meridional circulation in the Southern Ocean and found results similar to the numerical simulations of Döös and Webb (1994). An unspecified mixing or diabatic flux was assumed to accomodate mass exchanges between layers at the surface. Such diabatic effects are a part of the connection between flow, water masses, and stratification that we wish to investigate, and the air–sea flux estimates described here point to a significant role for surface fluxes rather than a negligible one.

Coarse resolution numerical models suggest that the strength of the Deacon cell is reduced when the advective effect of transient eddies is taken into account (Danabasoglu et al. 1994) to the extent that the cell may even be eliminated. This occurs because the eddies are expected to release potential energy and flatten isopycnals, causing a net eddy mass flux to the south in the surface layer that opposes the Ekman transport. The nature of the eddy mass flux near the surface is unclear, though, and even its direction may differ from the slumping scenario (Marsh et al. 1999) depending (in their parameterization) on the structure of the mixed layer. The fundamental point, however, is that the meridional cell in any model has to be compatible with buoyancy forcing, eddy transports, and mixing parameterizations of the model. Ocean models with weak buoyancy forcing (e.g., Döös and Webb 1994) necessarily have a weak cross-frontal or diabatic Deacon cell (Tandon and Garrett 1996), independent of the strength of the Ekman transport.

Marshall (1997) has shown how in a 2D ocean model the surface buoyancy flux condition sets the meridional overturning and, via an eddy flux parameterization, the interior stratification. A coupled air–sea model simulation (3D) with various eddy transport parameterizations demonstrates that different eddy transport physics leads to changes in stratification, air–sea exchange, and water mass transformation, and a new diabatic meridional circulation consistent with the transformation rate (Speer et al. 2000).

Southern Ocean transformation and stratification are analyzed here for the information they reveal about the strength and basic mechanism of the meridional circulation. The net effect of both the geostrophic transport and eddy transport, if significant, are contained in these quantities. The analysis is done in density classes and implies that if the interior flow is essentially adiabatic, the supply of mass to the surface layer is, to a large extent, from isopycnals, which are open across Drake Passage, and correspond to the low oxygen Upper Circumpolar Deep Water (UCDW: Callahan 1972). Webb (1993) has suggested that the Kerguelen Plateau provides a western boundary along which deep water might flow southward in the latitude range of Drake Passage. However, the plateau deepens to the south, and is too deep to block the UCDW in the latitude range of Drake Passage. Therefore interior, ageostrophic, eddy mass fluxes are suggested to supply mass to the surface Ekman layer, and partially to close the Deacon cell. The inference of a poleward flow of UCDW is consistent with tracer distributions showing low oxygen water originating in the deep Indian Ocean and Pacific Ocean (Callahan 1972), which spreads southward across the Circumpolar Current (ACC) and upwells beneath the westerly winds between the Polar Front and the Antarctic divergence. Potential vorticity and thickness gradients consistent with a southward eddy mass flux are found in these low-oxygen layers, and a simple parameterization is applied to estimate the strength of this transport.

2. Wyrtki's model and southward ageostrophic flow

A Sverdrup-dynamics sketch of the overall Southern Ocean circulation was presented by Stommel (1957), in which meridional boundaries idealized from real topography were added to the usual flat-bottom model. These could support western boundary currents, which close the interior flow driven by the wind. The meridional baroclinic circulation was supplied essentially by southward flow in a deep western boundary current along South America; however, the internal structure of the

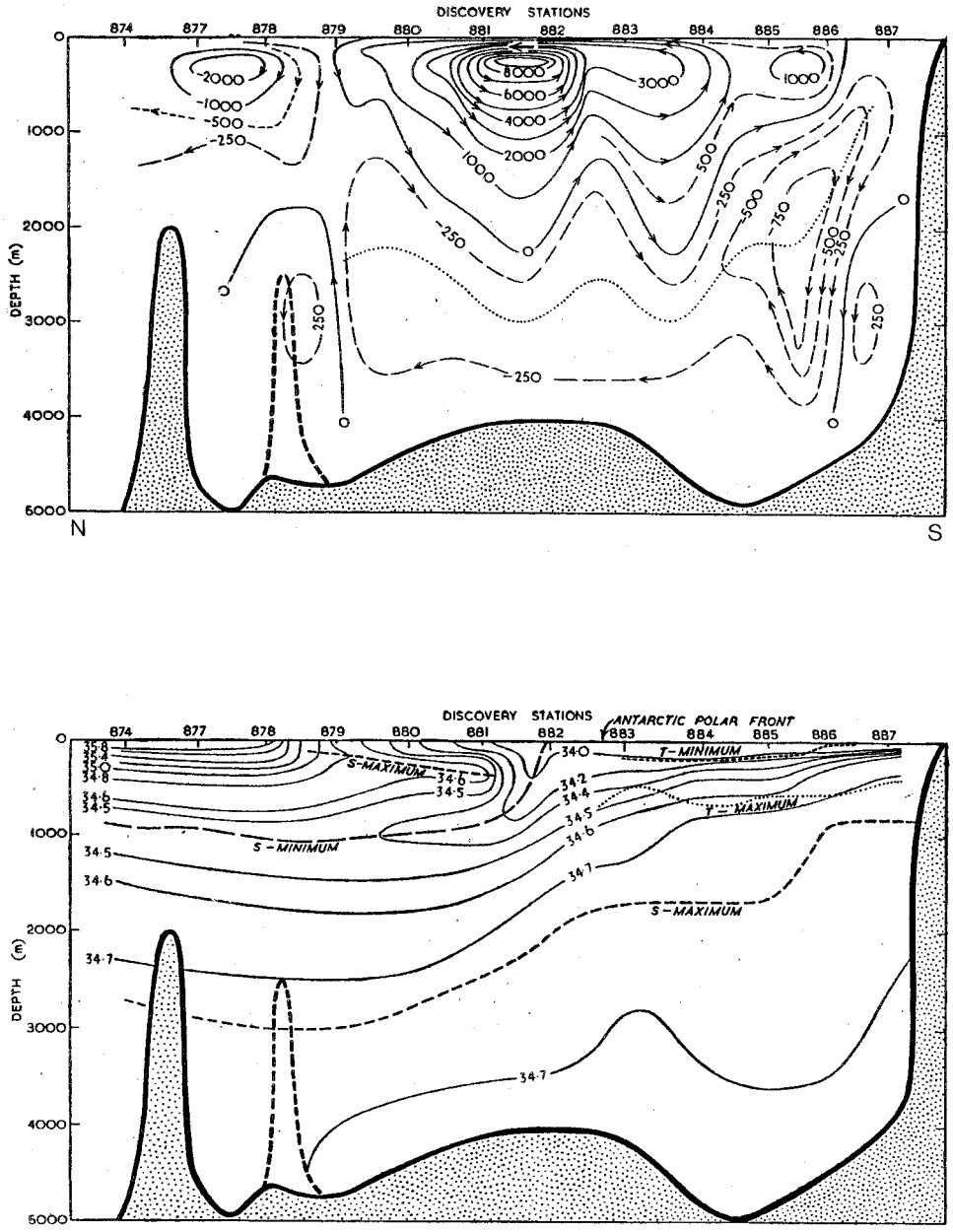

FIG. 2. *Discovery* section from Cape Leeuwin to Antarctica. (upper) Meridional streamfunction ($cm^2\ s^{-1}$) from Wyrtki (1960). Northward flow in a surface Ekman layer is compensated at depth; dotted line shows layer of no meridional motion. All meridional flow is ageostrophic in this model. (lower) Salinity distribution with position of temperature and salinity extrema; UCDW (T-max) and NADW (S-max).

circumpolar current was specified rather than calculated by setting the upwelling across interior level surfaces.

Wyrtki (1960) developed a frictional Sverdrup model, arguing that the purely Sverdrup model by Stommel (1957) could not explain the observed location of the current relative to the wind field, and had southward flow only south of the maximum westerlies (where there is vortex stretching), hence too far south to receive deep water from anywhere but the southwest Atlantic Ocean, whereas observations suggested a supply from other oceans as well. Furthermore, while the Sverdrup flow directs the current southward as observed, it does not help to get mass and properties across the Polar Front. Wyrtki (1960) addressed this issue and developed a model for the transverse circulation using a simple frictional damping proportional to velocity throughout the water column. This model implied southward flow below the Ekman layer broadly across the current and Polar Front, including in layers open at Drake Passage (Fig. 2). He arrived at an estimate for the southward

deep transport of 2.2 Sv, of which about 2 Sv is UCDW (temperature maximum, Fig. 2) that upwells south of the Polar Front. The North Atlantic Deep Water (NADW, salinity maximum) upwelling is mostly confined near the continent in an intense recirculation involving bottom water.

This southward subsurface flow was a purely mechanical affair, being flow down the north–south pressure gradient set up by the wind stress, at a rate proportional to the damping parameter. No consideration was given to the thermodynamical balance or heat fluxes implied by such flow in combination with the Ekman drift and other meridional flow in the model. We proceed to examine diagnostically the diabatic nature of the meridional flow and to show the relation between upwelling and surface forcing with simple models.

3. Air–sea forcing and transverse flow

The goal is to illustrate the necessary relationship between wind and buoyancy forcing in a simplified framework. Equations are written for the transport velocity U, the sum of Eulerian flow u, and the eddy mass flux u^* (Andrews et al. 1987), $V = v + v^*$, $U = u$, $W = w$:

$$-fV = \tau^w_z - fv^* \tag{1}$$

$$fU_z = -b_y \tag{2}$$

$$V_y + W_z = 0 \tag{3}$$

$$Vb_y + Wb_z = 0 \quad \text{interior} \quad \text{or}$$

$$Vb_y = \frac{B}{h_m} \quad \text{mixed layer,} \tag{4}$$

where f is the Coriolis parameter, B is the buoyancy flux, and h_m is the mixed layer thickness; a factor of ρ_o has been absorbed by τ, and $b = -g\rho/\rho_o$ is buoyancy. The wind stress $\tau^w(y, z = 0)$ drives an Ekman layer with structure $\tau^w(y, z)$. Using (3), $V = -\psi_z$, and $W = \psi_y$. Define a transformation by air–sea fluxes in this 2D model as $F_{2D} = B/b_y$.

Wyrtki's (1960) model has $fv^* = rU$ to include friction, parameterized as damping with the constant r, in the simplest manner. Then

$$\psi_z = f^{-1}(\tau^w_z - rU), \tag{5}$$

which, integrated over the constant-density mixed layer from $z = 0 = \psi(0)$ gives, with U_o the geostrophic velocity in this layer,

$$\psi_{\text{ml}} = Vh_m = f^{-1}(\tau^w - rh_mU_o) = F_{2D} \tag{6}$$

This connects the strength of the current U_o, the wind, and the buoyancy forcing or transformation. In this model there is a frictional transverse flow below the Ekman layer. Wyrtki derived the transverse flow V on a section across the Circumpolar Current using wind stress data, ignoring the buoyancy equation and regarding $U(z)$ as given by hydrography b and reference level choices.

To complete the solution, match $\psi_{\text{ml}}(y)$ to the adiabatic interior streamfunction $\psi(b(y))$ from (4). In terms of b, $d\psi/db = f^{-1}rU(b)/b_z$. Then

$$\psi = \frac{-r}{f}\int_{\text{ml}}^{b} \frac{U}{b_z}\,db + \psi_{\text{ml}}(b). \tag{7}$$

The essential physics of the transverse circulation is the presence of friction in the interior, giving rise to a southward ageostrophic cross-frontal flow below the Ekman layer, hence upwelling along deeper isopycnals, which rise toward the surface owing to thermal wind (b_y) in the Circumpolar Current.

Another choice for friction is $fv^* = -rU_{zz}$. This choice implies that

$$\psi = f^{-1}\left(\tau^w - \frac{r}{f}b_y\right) + F_{2D}, \tag{8}$$

where the total Ekman plus eddy transports again balance surface forcing. With significant surface forcing or transformation r is smaller than the scale $r = f\tau^w/SN^2$, where S is isopycnal slope and N is the buoyancy frequency. Gent et al. (1995) showed how their eddy mass flux parameterization leads to a similar form for friction after some approximation (see also Tandon and Garrett 1996), and Marshall (1997) has applied this parameterization to a model of the transverse circulation in the Southern Ocean, showing how the density field adapts to satisfy the thermodynamic balance (4) with eddy fluxes. This parameterization of friction is more physically motivated than simple damping (when Reynolds stresses are negligible) since it can be related to thickness or potential vorticity gradients on isopycnals, the underlying idea being the lateral mixing of potential vorticity by eddies, which modifies the thermal wind and acts as an effective vertical viscosity.

4. Transformation

The transformation rate F from one density class to another due to air–sea heat and freshwater fluxes may be combined with that due to mixing D_b and advection A in the equation (Walin 1982; Speer 1997)

$$F - A - \frac{\partial D}{\partial b} = 0 \tag{9}$$

$$F(b) = \int_{\text{year}} dt \iint_{\text{area}} -B\,dx\,dy \times \delta[b(x, y, t) - b'] \tag{10}$$

with the buoyancy flux

$$B = -\frac{g\alpha}{\rho_o C_p}\mathcal{H}(x, y, t) + \frac{g\rho(T, 0)\beta S}{\rho_o(1 - S)}\mathcal{W}(x, y, t), \tag{11}$$

where $\mathcal{H}(x, y, t)$ and $\mathcal{W}(x, y, t)$ are the surface fluxes of

heat and freshwater (evaporation minus precipitation), g is gravity, α is the thermal expansion coefficient, and C_p is the specific heat of seawater. Both surface fluxes are functions of location and time, assumed to vary periodically with the seasonal cycle. Given the temperature and salinity of the surface water $T(x, y, t)$ and $S(x, y, t)$, it is possible to calculate the buoyancy flux as function of the surface buoyancy. The delta function appearing in the integral is zero whenever the surface buoyancy b' is not equal to the buoyancy b, and therefore samples the surface flux only for surface water of buoyancy b. Dividing by one year yields the annual average. For convenience, $F(b)$ or $F(\rho)$ is called the transformation by air–sea fluxes and its derivative with respect to buoyancy or density the formation.

Define the net advective volume flux A and the diffusive flux D by their integral along an isopycnal from a control surface to the sea surface:

$$A = \int_b (\mathbf{u} \cdot \mathbf{n})\, dS, \tag{12}$$

where $\mathbf{n}$ is the unit normal vector to isopycnals, $\mathbf{u}$ is the velocity, and dS is the isopycnal surface area element, and

$$D = \int_b -\kappa \frac{\partial b}{\partial n}\, dS, \tag{13}$$

where κ is the diapycnal diffusivity.

The derivative of the diffusive flux D with respect to density or buoyancy appears in the transformation equation (only variations in D contribute to cross-isopycnal mass transport). Some aspects of air–sea transformation F (Fig. 3) have been discussed by Speer et al. (1997) for the information it provides about the formation rate of subantarctic mode water ($26 \leq \gamma \leq 27$) in different basins. Here, the emphasis is on the existence of net buoyancy gain over high-latitude density classes (Fig. 3) and the relation to upwelling deep water.

A key observation is net buoyancy gain near and south of the Polar Front (surface density $\gamma \sim 27$). Taylor et al. (1978) remarked substantially on this point using datasets covering regions south of Australia and in the southern South Atlantic Ocean, in their search for mechanisms to explain the front. They concluded that neither the air–sea heat flux nor the Ekman drift were directly responsible for creating the Polar Front at the surface, but that it was rather the result of larger-scale motion associated with divergent Ekman flow (Fig. 3; see also Wyrtki 1960). However, the presence of the Polar Front was thought to be at the origin of the buoyancy gain zone on its southern side, as meandering ocean and atmosphere flows could lead to a net transfer of heat from warmer subantarctic air to underlying Antarctic surface water. Episodic outbreaks of warm air south of the Polar Front may play a role as well. The Taylor et al. (1978) study did not address the connection of this buoyancy gain to northward Ekman transport (e.g., Toole 1981). Warren et al. (1996), on the other hand, noted the agreement between Ekman transport across 60°S and heat and freshwater balances derived from various estimates; furthermore, they arrived at net buoyancy gain at high latitudes for several choices of datasets.

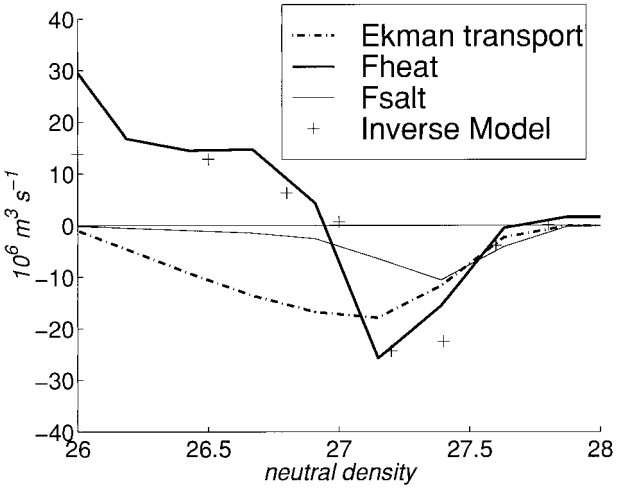

FIG. 3. Transformation in the Southern Hemisphere from COADS heat flux data (heavy solid; negative values are buoyancy gain by the ocean). An estimate of the freshwater flux contribution to transformation based on an adjusted COADS freshwater flux is shown (light solid; the adjustment is essentially a reduction by 1–2 mm day^{-1} at high latitudes to bring the mean closer to other climatologies). A zone of buoyancy gain occurs at densities higher than 27 in both components of buoyancy flux. Ekman transport is shown for comparison, showing the alignment of buoyancy gain and growing northward Ekman transport (divergent Ekman flow). Inverse model results for total transformation show a basic compatibility with buoyancy gain. Transformation from heat flux alone changes sign near 27.8, but is more than compensated by that due to freshwater flux. Values at densities near 28 and higher are not resolved.

While oceanic heat gain at high southern latitudes at first may seem surprising, it reflects the different geometry of the Northern and Southern Hemispheres. In the Northern Hemisphere, vast quantities of heat are removed from the ocean in outbreaks of cold, dry, continental air over the western boundary of the ocean where western boundary currents carry warm water poleward. Although outbreaks occur near continental boundaries in the Southern Hemisphere, much of the Southern Ocean is far from continents, air and sea surface temperatures are more nearly aligned with one another, and the seasonal cycle is muted. Any heat exchange with the atmosphere happens mainly in departures from the rough zonal symmetry, with colder waters south of the front tending to gain heat in north–south excursions that are out of phase with atmospheric flow.

Our transformation curve (Fig. 3) illustrates that Ekman transport and transformation are consistent with one another over the surface density range of $27.2 \leq \gamma \leq 28$ (or $27 \leq \sigma \leq 27.8$) corresponding to the zone south of the Polar Front. Note that, if the net meridional eddy mass flux in the surface layer were substantially opposed to the Ekman layer transport, the transforma-

tion would be very weak and the two would not agree [in the absence of significant horizontal diffusive buoyancy flux in the surface layer; cf. (9) with $A = D = 0$]. In our analysis the transformation and Ekman transport are similar across the Circumpolar Current, and surface eddy mass transport is not evident. To the north of the current at subantarctic mode water (SAMW) densities the two quantities differ considerably. Here, other mechanisms including gyres and western boundary currents become important for meridional flow.

The maximum heat flux associated with the zone of buoyancy gain is about 30 W m^{-2} in the Comprehensive Ocean Atmosphere Data Set (COADS) data. Bunker's (1988) estimates were up to 40 W m^{-2} heat gain by the ocean in the South Atlantic sector, and Taylor et al. (1978) found 35 W m^{-2} heat gain south of Australia. These maximum values are significant in a region with errors likely to be several tens of W m^{-2}; however, average values at many latitudes are statistically quite dubious. Although the winds and fluxes in the COADS data are self-consistent, the observations on which it is based are sparse in space and in time (zonal symmetry compensates somewhat for the former defect). In particular, we have to accept complete ignorance of average fluxes at the highest latitudes near ice, and no use of the data is made for the highest surface density classes, near $\gamma = 28$. This is nevetheless the best dataset available to us. Some confidence in the observed transformation rates may be gained from the results of an inverse model (Fig. 3) that show a basic compatibility between COADS heat fluxes and geostrophic and Ekman flow across 30°S and between the principal ocean basins (Sloyan and Rintoul 2000).

An estimate of transformation from COADS freshwater fluxes (F_{salt}) displayed with the heat flux based value (Fig. 3), shows that F_{salt} also contributes significantly to a net buoyancy gain by the Southern Ocean. However, we are not confident enough in the value to include it for an estimate of total transformation based on COADS data alone. The simple estimates outlined above, along with inverse model solutions (Sloyan and Rintoul 2000) and coupled air–sea model solutions (Speer et al. 2000), all lead to substantial buoyancy gain at high southern latitudes.

The increasing transformation from $\gamma = 28$ to $\gamma = 27.2$ requires a mass source in the same density classes (9). From Fig. 1 we see that these density classes are those of UCDW and a part of the Antarctic Intermediate Water (AAIW), implying that these water masses upwell to feed northward transport near the surface. This contrasts with the usual view that upwelling NADW feeds the northward transport. Our analysis shows that the upper branch of the meridional overturning cell is supplied by the upwelling of UCDW, which subsequently participates in northward Ekman flow, with the required transformation accomplished by air–sea fluxes. Mixing can corrupt a simple relation between transformation and upwelling along isopycnals from deep to surface layers, but standard mixing coefficients would have to be greater than 1 $cm^2\ s^{-1}$ (vertical) or $10^6\ cm^2\ s^{-1}$ (horizontal) to have much effect. Note that air–sea fluxes that are density or buoyancy compensating (e.g., cooling and freshening) likely play a role in converting UCDW to cool, fresh Antarctic surface water in the same density classes. (Such conversions could also be examined quantitatively in a similar framework to that presented here, and the relative contribution of isopycnal mixing in changing the T and S of upwelling water might be assesed.)

If isopycnal upwelling of UCDW is a significant source of mass to regions south of the Polar Front we are confronted with the problem, outlined earlier, of how to get a net transport of water across the Circumpolar Current, and in particular across the latitudes of Drake Passage. The other major north–south barrier, the Kerguelen Plateau, is too deep at the latitudes of Drake Passage to block this water mass, although it does provide a western boundary for denser layers. Warren (1990) has even used the constraint of no net geostrophic flow across Drake Passage latitudes on density surfaces in the UCDW to explain its worldwide low oxygen concentrations. Upwelling does not conflict with the low oxygen concentrations, but an ageostrophic mechanism for transport is required. Based on the arguements for an eddy mass transport outlined earlier, potential vorticity and thickness gradients are examined next in deep layers.

5. Observed potential vorticity gradients

A section of average hydrographic properties south of Australia was constructed from six repeated occupations of WOCE section SR3 from Tasmania to Antarctica (Rintoul and Bullister 1999), during different seasons and different years (Fig. 1). Data were gridded on a ½° latitude interval and averaged in (neutral) density bins ($\Delta\gamma = 0.1$) to preserve vertical structure.

Large-scale potential vorticity is defined here for convenience as hf_o/f, where f_o is the Coriolis parameter at 45°S, and h is the thickness of $\Delta\gamma = 0.1$ density bins (Fig. 4: this definition has units conveniently similar to thickness). The dominant structure is the thick SAMW layer in the northern part of the section centered at about $\gamma = 26.9$. Below this layer, little structure exists until the UCDW layer 27.5–27.9. From 27.9–28.1 the NADW stands out with somewhat thicker PV but quite uniform in latitude. Values near the bottom and surface are dominated by noisy topographic and mixed layer effects. The principal large-scale PV gradient occurs in the UCDW layer, with equivalent thickness variations of several hundred meters, and decreasing thickness to the south.

The circumpolar nature of this PV gradient is illustrated using a climatological dataset from the Hamburg Special Analysis Center (HSAC). This dataset was generated using isopycnal averaging from historical ar-

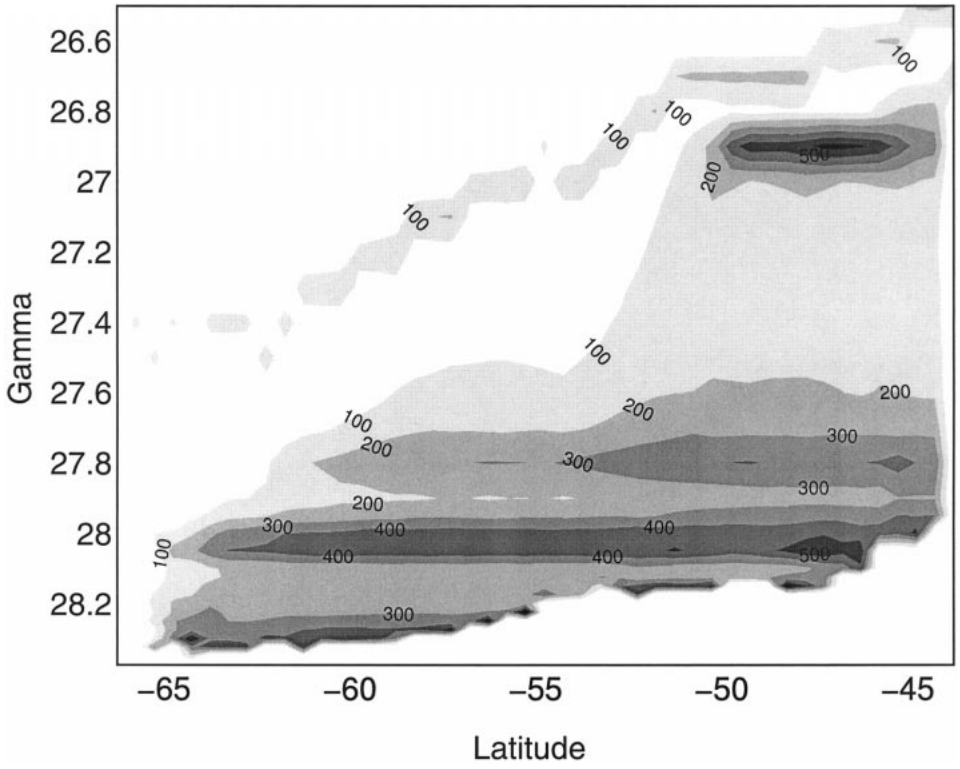

FIG. 4. Averaged section potential vorticity (m, definition in text) between isopycnal layers separated by 0.1γ. Subantarctic mode water stands out near 26.9, other layers are AAIW: 27–27.5, UCDW: 27.5–28, NADW: 28–28.2, and AABW below 28.2.

chives (Gouretski and Jancke 1998). Zonally averaged thickness (Fig. 5) shows the dominant gradient in UCDW, along with a similar, but factor of 2 weaker, gradient over a more restricted latitude range in the AAIW. North of about 60°S, that is, in the major frontal regions of the Southern Ocean, NADW thickness is rather more uniform, increasing slightly to the north (tending to compensate a decreasing f).

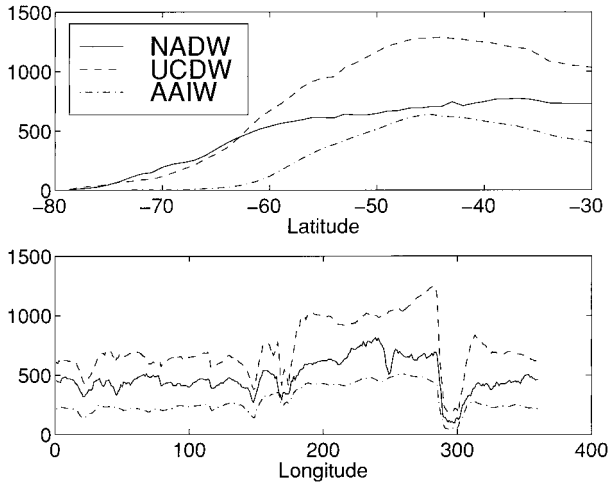

FIG. 5. Circumpolar average thickness from the Hamburg SAC climatology in several layers. Plotted vs latitude (upper) and versus longitude (lower) south of 30°S. Thickness versus longitude is dominated by bottom depth variations.

The detailed distribution of PV in the three principal layers from the HSAC climatology is displayed (Fig. 6) to show the tight relationship between PV and Southern Ocean fronts, as defined by Orsi et al. (1995). For the mean Eulerian flow this suggests approximate conservation of PV as water circulates around Antarctica in the main cores of the ACC.

The NADW layer shows substantial areas of uniform PV, roughly bounded by the Subantarctic Front and Polar Front (Fig. 6c). That this layer should exhibit more homogenization than overlying layers seems at first puzzling since it receives water with a range of PV from the South Atlantic Ocean. However, this situation likely reflects the absence of the Drake Passage constraint on the bulk of this layer. Thus shallower layers can satisfy PV conservation at lowest order by circumpolar motion along open geostrophic contours, whereas NADW evolves to a state with PV homogenization at about its average Southern Ocean value.

Relatively uniform PV appears in the AAIW layer as well, but only to the north of the frontal zones, well within the southern subtropical gyres (Fig. 6a). The values are quite different in the Pacific Ocean, where PV is lower compared to the Atlantic Ocean or Indian

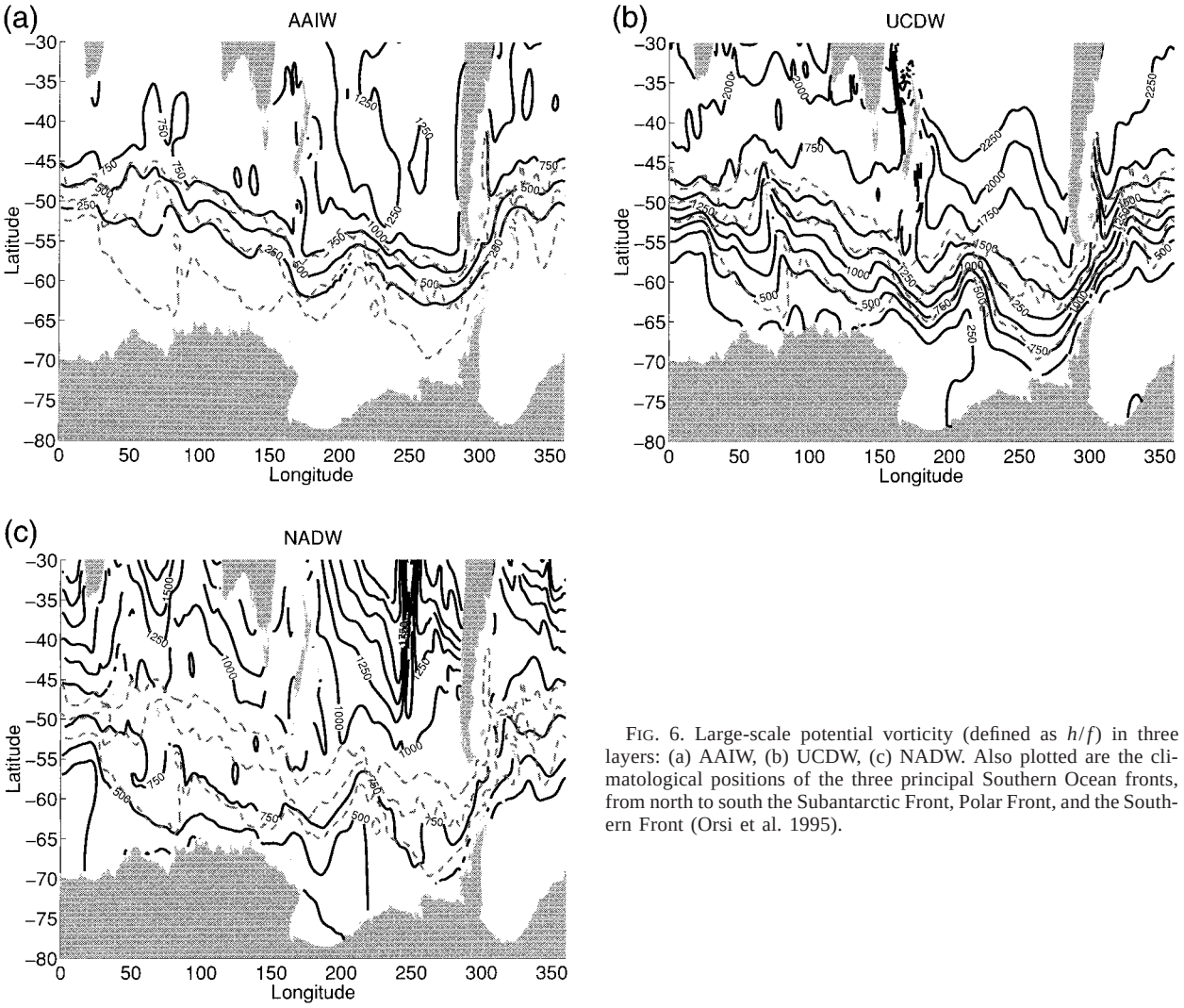

FIG. 6. Large-scale potential vorticity (defined as h/f) in three layers: (a) AAIW, (b) UCDW, (c) NADW. Also plotted are the climatological positions of the three principal Southern Ocean fronts, from north to south the Subantarctic Front, Polar Front, and the Southern Front (Orsi et al. 1995).

Ocean, suggesting that the processes that supply and fill these basins (Talley 1995) are not the same. A gradient exists across the frontal zones, where this layer rises to the surface near the Polar Front. In the circumpolar frontal region isopleths of PV in both AAIW and UCDW layers are closely aligned except for the area surrounding the Kerguelen Plateau. The deeper layer is strongly influenced by the topography of the plateau, and the PV pattern changes abruptly.

6. Southward eddy transport

a. Strength and vertical structure

The interior ageostrophic meridional flow, with the previous parameterization

$$v^* = \frac{r}{f} U_{zz} = \frac{r b_{yz}}{f^2}. \tag{14}$$

Rewriting this for interior isopycnal layers of thickness h defined by a buoyancy interval Δb:

$$v^* = \frac{-r\Delta b}{f^2 h^2} \frac{\partial h}{\partial y} = -\frac{\kappa}{h} \frac{\partial h}{\partial y}, \tag{15}$$

where $r = \kappa f^2/N^2 = \kappa f^2 h/\Delta b$ has been substituted for convenience to have a lateral mixing coefficient κ as the frictional control parameter (e.g., Gent et al. 1995).

From our data the scale for v^* may be estimated as $\kappa/\Delta y$ since $h = 10^2$ m and Δh are of similar size. So $v^* = 10^{-3}$ m s^{-1}, with $\kappa = 10^3$ m^2 s^{-1} and $\Delta y = 10^6$ m. Over a circumpolar length scale of 10^4 km this implies a net southward transport within the layer of the order of 10^6 m^3 s^{-1}. Adding up ten such layers over Upper Circumpolar Deep Water, the total southward transport is about 10×10^6 m^3 s^{-1}.

In these layers the internal stress can be found by integrating $\tau_z = fv^*$, so the stress difference across a

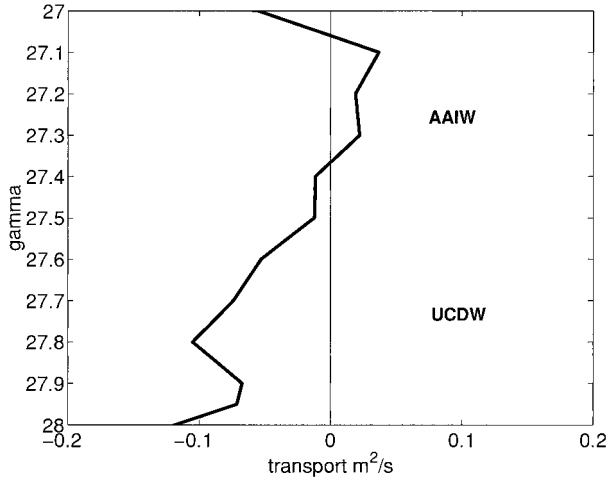

FIG. 7. Layer transport (hv^* in $m^2\ s^{-1}$, negative values south) based on an eddy mass flux parameterization ($\kappa = 1000\ m^2\ s^{-1}$; see text). Estimates based on a meridional average excluding boundaries over the SR3 (averaged) section.

layer of thickness h is $\Delta\tau = fhv^*$, where $\Delta\tau$ is now a function of density. From the previous discussion we expect the stress divergence to be maximum across the UCDW layer.

Thickness data from the averaged SR3 section together with (15) can be used to construct the vertical structure of v^* (Fig. 7). [Circumpolar average gradients from the HSAC climatology are similar (Fig. 5), and we prefer here to use the results from averaged high resolution sections at the same location.] Values have been averaged meridionally across the frontal zone to represent better the net southward flow. A southward eddy transport of 0.1 $m^2\ s^{-1}$ emerges in deep layers spanning UCDW, again using a coefficient of $10^3\ m^2\ s^{-1}$. Summing over five layers ($\Delta_\gamma = 0.1$) gives a zonally integrated total of about 5–10 ($\times 10^6\ m^3\ s^{-1}$) of southward transport, enough to compensate virtually all of the Ekman transport in the UCDW density range and one half of the total northward Ekman transport.

The dependence of these numbers on a mixing coefficient means that we have only a scale for the total transport. If $100 \leq \kappa \leq 1000\ m^2\ s^{-1}$ is the plausible range, based on numerous tracer and both direct and indirect velocity estimates (e.g., Keffer and Holloway 1988), then total transport lies within 1–10 ($\times 10^6\ m^3\ s^{-1}$). However, unless κ varies strongly with depth the vertical structure found here is independent of the mixing coefficient. Most fundamentally, the PV gradients in UCDW layers do exist, and any lateral PV mixing at all produces southward mass transport.

With the parameterization used here, some southward transport in the AAIW layer would appear using the HSAC circumpolar climatology, though gradients are weaker and the layer is thin, so the net transport is small. Both air–sea transformation (Fig. 3: Speer et al. 1997) and geostrophic transport calculations (Sloyan and Rintoul 2000) imply little net north–south exchange in the AAIW layer.

The time and length scales over which this PV mixing occurs is not clear. Direct observations of eddy fluxes are sparse in the Southern Ocean. Where long time series of measurements do exist, for example, in Drake Passage (Johnson and Bryden 1989) or south of Australia (Phillips and Rintoul 2000), poleward eddy heat flux is found to decrease with depth. This is equivalent to a divergence of the interfacial form stress of the sign to drive an *equatorward* meridional flow at intermediate depths, that is, of the opposite sign to that expected from the large-scale gradient of the potential vorticity. A resolution of this apparent contradiction may be provided by the role of standing topographic eddies. Using the FRAM model, Stevens and Ivchenko (1997) find that interfacial form stress is dominated by the standing eddy component, mainly associated with large-scale meanders of the Circumpolar Current, and that the net flux due to transient eddies is small.

b. Other transport processes

At densities 27.2–27.4 more water is being blown northward near the surface than can be supplied by the southward subsurface isopycnal eddy mass flux (Fig. 3 and Fig. 7). But these lower density isopycnals outcrop north of Drake Passage, so a net geostrophic flow near the surface across isopycnals can simply supply the Ekman transport. This may be true to some degree on denser isopycnals as well, but further calculations are needed to isolate this component.

The diffusive term D, if significant, confounds a simple relation between transformation F and advection A. With or without D the Ekman transport must be supplied somehow, but the relation to air–sea buoyancy fluxes would no longer be direct if diffusion were very important. The divergence of the transformation from the Ekman transport observed at $\gamma = 27$ (Fig. 3), or roughly at the transition to SAMW densities, may reflect stronger mixing processes as well as a geostrophic contribution in the southern part of subtropical gyres and the poleward extension of western boundary currents.

7. Discussion

Transformation calculations suggest that a significant upwelling of deep water occurs in UCDW layers, forming a shallower upper meridional cell than one based solely on the upwelling of NADW. The UCDW layers are open across Drake Passage, and an ageostrophic southward flow is needed to close the cell. Hydrographic observations indicate strong north–south PV gradients in the UCDW layer, which in the strong flow of the circumpolar frontal region means that eddy stirring, perhaps by standing eddies, can transport mass southward. Transformation rates, Ekman transport, and eddy-driven

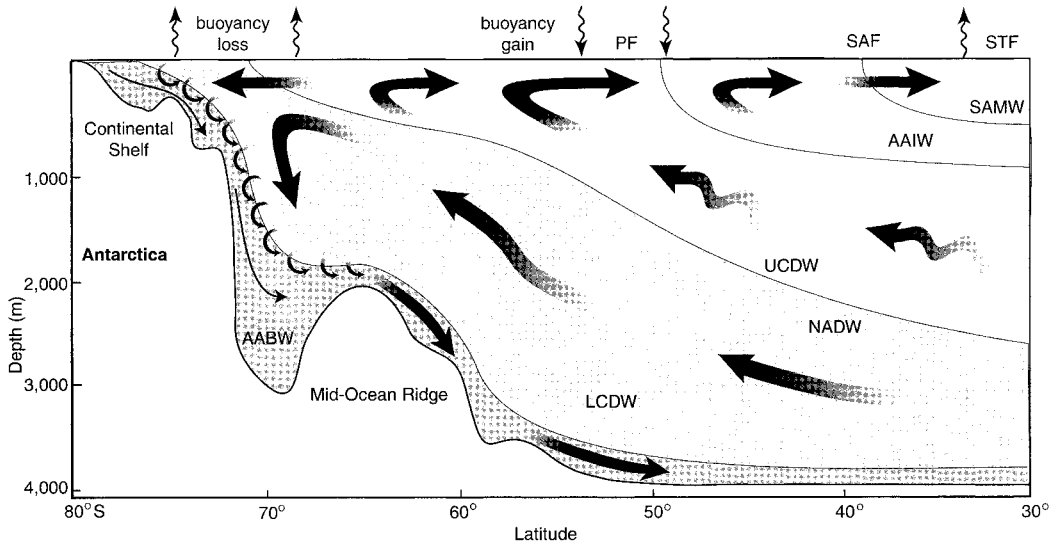

FIG. 8. Schematic two-cell meridional overturning circulation in the Southern Ocean. An upper cell is primarily formed by northward Ekman transport and southward eddy transport in the UCDW layer. A lower cell is primarily driven by dense water formation near the Antarctic continent.

mass transports are shown to be consistent with an UCDW cell (Fig. 8).

A strong southward transport of NADW occurs as well, but the flow can be geostrophic because deep ridges cross the circumpolar zone; this water mass is primarily returned northward as dense bottom water. The amplitude of the deep NADW and bottom water cell is determined by buoyancy loss at high density (not resolved here) and by entrainment, and can be to some extent independently large compared to the upper cell.

While southward eddy mass transport in the UCDW layers solves the paradox of upwelling in layers open across Drake Passage, the true strength and vertical distribution of the flow is not well determined. The spatial distribution of Lagrangian displacement, for instance in fronts or downstream of topography may give some hints about the mechanism of southward transport in each layer.

The contribution of each ocean to the meridional circulation within the circumpolar current also remains unclear. The concept of a more uniformly circumpolar tranverse circulation was proposed by Sverdrup (1933), and Wyrtki's (1960) model was a simple dynamical framework for such a circulation. But the degree of uniformity very likely differs from layer to layer. Southward deep flow at latitudes bounded by continents from all three oceans has been described in regional studies (Warren 1973; Toole and Warren 1993; Saunders and King 1995) and global studies (Macdonald 1993; Sloyan and Rintoul 2000). Such studies do not, however, necessarily determine meridional transfers farther south, across the Polar Front, for instance.

The total southward flow can be large. Sloyan and Rintoul (2000) estimated a zonally integrated total southward geostrophic transport of about 50 Sv. This inflow has to compensate not only the 20–25 Sv of buoyant transformation or Ekman transport found here, but also the deep water that has been entrained and exported in bottom water. If the bottom water exported is roughly double the net formation of very dense water on the continental shelf, say 5–10 Sv (Orsi et al. 1999), then the total (30–45 Sv) is not far from the amount required. The contraints on circulation provided by the analysis presented here also suggest a rather circuitous return route for the NADW. After leaving the Atlantic Ocean, and filling deep layers in the Indian and Pacific Oceans, it outcrops close to the Antarctic continent, where cooling and brine rejection convert some of it to bottom water—the lower branch of the meridional cell. Only after being converted to UCDW by mixing in basins farther north is the water able to move south across the ACC at lower densities, outcrop, and be blown north and converted to still lower densities, finally reentering the Atlantic as intermediate water, mode water, and other shallow components. The buoyant transformation in the Southern Ocean provides for the ultimate closure of the thermohaline return flow in a diabatic Deacon cell.

Acknowledgments. Support for this study was received from the CNRS, CSIRO, and Environment Australia through the National Greenhouse Research Program. We thank Tony Hirst for helpful comments on the manuscript.

REFERENCES

Andrews, D. B., J. R. Holton, and C. B. Leovy, 1987: *Middle Atmosphere Dynamics.* Academic Press, 489 pp.

Bunker, A. F., 1988: Surface energy fluxes of the South Atlantic Ocean. *Mon. Wea. Rev.,* **116,** 809–823.

Callahan, J. E., 1972: The structure and circulation of Deep Water in the Antarctic. *Deep-Sea Res.,* **19,** 563–575.

Danabasoglu, G., J. C. McWilliams, and P. Gent, 1994: The role of mesoscale tracer transport in the global ocean circulation. *Science,* **264,** 1123–1126.

da Silva, A. M., C. C. Young, and S. Levitus, 1994: *Atlas of Surface Marine Data 1994.* Vol. 3: *Anomalies of Heat and Momentum Fluxes.* NOAA Atlas NESDIS 8, U.S. Department of Commerce, NOAA, NESDIS.

Deacon, G. E. R., 1937: The hydrology of the Southern Ocean. *Discovery Reports,* **15,** 1–124, plates I–XLIV.

Döös, K., 1994: Semianalytical simulation of the meridional cells in the Southern Ocean. *J. Phys. Oceanogr.,* **24,** 1281–1293.

——, and D. Webb, 1994: The Deacon cell and other meridional cells of the Southern Ocean. *J. Phys. Oceanogr.,* **24,** 429–442.

Gent, P. R., J. Willebrand, T. McDougall, and J. C. McWilliams, 1995: Parameterizing eddy-induced tracer transports in ocean circulation models. *J. Phys. Oceanogr.,* **25,** 463–474.

Gouretski, V., and K. Jancke, 1998: A new world ocean climatology: Objective analysis on neutral surfaces. Tech. Rep. 3, WHP Special Analysis Center, Hamburg, Germany, 12 pp.

Johnson, G. C., and H. L. Bryden, 1989: On the size of the Antarctic Circumpolar Current. *Deep-Sea Res.,* **36,** 39–53.

Keffer, T., and G. Holloway, 1988: Estimating Southern Ocean eddy flux of heat and salt from satellite altimetry. *Nature,* **332,** 624–626.

Macdonald, A. M., 1993: Property fluxes at 30°S and their implications for the Pacific–Indian throughflow and the global heat budget. *J. Geophys. Res.,* **98,** 6851–6868.

Marsh, R., A. J. G. Nurser, A. P. Megann, and A. L. New, 2000: Water mass transformation in the Southern Ocean of a global isopycnal coordinate GCM. *J. Phys. Oceanogr.,* **30,** 1013–1045.

Marshall, D., 1997: Subduction of water masses in an eddying ocean. *J. Mar. Res.,* **55,** 201–222.

Orsi, A., T. Whitworth, and W. Nowlin, 1995: On the meridional extent and fronts of the Antarctic Circumpolar Current. *Deep-Sea Res. I,* **42** (5), 641–673.

——, G. C. Johnson, and J. L. Bullister, 1999: Circulation, mixing, and production of Antarctic Bottom Water. *Progress in Oceanography,* Vol. 43, Pergamon, 55–109.

Phillips, H. E., and S. R. Rintoul, 2000: Eddy variability and energetics from direct current measurements in the Antarctic Circumpolar Current south of Australia. *J. Phys. Oceanogr.,* **30,** 3050–3076.

Rintoul, S. R., and J. Bullister, 1999: A late winter hydrographic section between Tasmania and Antarctica. *Deep-Sea Res.,* **46,** 1417–1454.

Saunders, P. M., and B. A. King, 1995: Oceanic fluxes on the WOCE A11 section. *J. Phys. Oceanogr.,* **25,** 1942–1958.

Sloyan, B. M., and S. R. Rintoul, 2000: The Southern Ocean limb of the global deep overturning circulation. *J. Phys. Oceanogr.,* in press.

Speer, K. G., 1997: A note on average cross-isopycnal mixing in the North Atlantic Ocean. *Deep-Sea Res.,* **44,** 1981–1990.

——, S. Rintoul, and B. Sloyan, 1997: Subantarctic mode water formation by air–sea fluxes. *Int. WOCE Newsl.,* **29,** 29–31.

——, E. Guilyardi, and G. Madec, 2000: Southern Ocean transformation in a coupled model with and without eddy mass fluxes. *Tellus,* in press.

Stevens, D. P., and V. O. Ivchenko, 1997: The zonal momentum balance in an eddy-resolving general-circulation model of the Southern Ocean. *Quart J. Roy. Meteor. Soc.,* **123,** 929–951.

Stommel, H., 1957: A survey of ocean current theory. *Deep-Sea Res.,* **4,** 149–184.

Sverdrup, H. U., 1933: On vertical circulation in the ocean due to the action of the wind with application to conditions within the Antarctic Circumpolar Current. *Discovery Reports,* VII, 139–170.

——, M. W. Johnson, and R. H. Fleming, 1942: *The Oceans: Their Physics, Chemistry, and General Biology.* Prentice-Hall, 1087 pp.

Talley, L. D., 1995: Antarctic Intermediate Water in the South Atlantic. *The South Atlantic: Present and Past Circulation,* G. Wefer et al., 219–238.

Tandon, A., and C. Garrett, 1996: On a recent parameterization of mesoscale eddies. *J. Phys. Oceanogr.,* **26,** 406–411.

Taylor, H. W., A. L. Gordon, and E. Molinelli, 1978: Climatic characteristics of the Antarctic Polar Zone. *J. Geophys. Res.,* **83,** 4572–4578.

Toggweiler, J. R., and B. Samuels, 1993. Is the magnitude of the deep outflow from the Atlantic Ocean actually governed by Southern Hemisphere winds? *The Global Carbon Cycle,* M. Heimann, Ed., NATO ASI Series, Springer-Verlag, 303–331.

Tomczak, M., and J. S. Godfrey, 1994: *Regional Oceanography: An Introduction.* Pergamon, 422 pp.

Toole, J. M., 1981: Sea ice, winter convection, and the temperature minimum layer in the Southern Ocean. *J. Geophys. Res.,* **86,** 8037–8047.

——, and B. A. Warren, 1993: A hydrographic section across the Subtropical South Indian Ocean. *Deep-Sea Res.,* **40,** 1973–2019.

Walin, G., 1982: On the relation between sea-surface heat flow and thermal circulation in the ocean. *Tellus,* **34,** 187–195.

Warren, B. A., 1973: Transpacific hydrographic sections at Lats. 43°S and 28°S: The SCORPIO expedition—II. Deep water. *Deep-Sea Res.,* **20,** 9–38.

——, 1990: Suppression of deep oxygen concentrations by Drake Passage. *Deep-Sea Res.,* **37,** 1899–1907.

——, J. H. LaCasce, and P. E. Robbins, 1996: On the obscurantist physics of ''form drag'' in theorizing about the Circumpolar Current. *J. Phys. Oceanogr.,* **26,** 2297–2301.

Webb, D. J., 1993: A simple model of the effect of the Kerguelen Plateau on the strength of the Antarctic Circumpolar Current. *Geophys. Astrophys. Fluid Dyn.,* **70,** 57–84.

Wyrtki, K., 1960: The Antarctic circumpolar current and the Antarctic polar front. *Dtsch. Hydrogr. Z.,* **13** (4), 153–174.